

NUMERICAL SIMULATIONS OF PENETRATION INTO POROUS GRANULAR TARGETS. K. Wada¹ and A. M. Nakamura², ¹PERC, Chiba Institute of Technology, Tsudanuma 2-17-1, Narashino, Chiba 275-0016, Japan (wada@perc.it-chiba.ac.jp), ²Graduate School of Science, Kobe University, Japan.

Introduction: Recent exploration missions to asteroids have revealed that small asteroids possess many features related to impact processes on their surfaces. Even on the surface of very small (<500m) asteroid Itokawa, we see regolith layers composed of fine pebbles or dust, crater-like circular depressions, large boulders, and dimple structures around rocks [1-6]. In order to understand forming mechanisms of these features and to clarify the evolution of asteroids, we need to reveal the impact cratering process on the asteroidal surfaces. We have not yet, however, obtained a set of complete scaling relations applicable to the asteroidal surfaces because of the properties particular to asteroids: asteroidal surfaces are covered with regolith layers that are expected to have a large porosity due to micro gravity of asteroids. Furthermore, not a few asteroids are expected to have a rubble pile structure, which is an aggregate of many fragments bounded by small gravity and thus a kind of porous granular materials. We have not yet fully understood the impact physics on such porous granular targets under micro gravity. One reason of this unclearness is that the role of porosity is not fully comprehended [7, 8]. Another reason is that cohesion between granular particles due to the van der Waals force becomes dominant under micro gravity. This adhesive force not only makes porous layers but also affects the impact cratering process [9-11]. Impact process on porous granular targets under micro gravity and its scaling relations should be elucidated for understanding evolution of asteroids.

In this study, we carry out numerical simulations of impacts into porous granular targets under micro gravity with using a kind of N -body code, Distinct Element Method (DEM) [e.g., 11, 12]. The impact velocities in our simulations are less than several 100 m/s, which are relatively low but enough to form various impact features on the asteroidal surfaces. Here, in particular, we focus on the penetration process of projectiles and penetration resistance acting on them. Previous laboratory studies revealed resistance laws for penetration into sand under 1G [13], aerogel [14], or highly porous sintered glass beads [15]. However, the resistance law for penetration into porous granular targets under micro gravity is not well understood so far, although some laboratory experiments are ongoing. We will obtain the penetration resistance law from our numerical simulations and compare them with those obtained from experiments.

DEM Model: In our DEM model, the mechanical interaction forces between contact spherical particles are expressed by elastic force and friction modeled by the Voigt-model, which consists of a spring and dash-pot pair. The spring gives elastic force based on the Hertzian elastic contact theory. The dash-pot expresses energy dissipation during contact to realize inelastic collision with a given coefficient of restitution e . For the tangential direction between contact particles, a friction slider is introduced to express Coulomb's friction law with a given coefficient of friction μ . As an adhesion model, we simply assume a constant attractive force F_a . This adhesive force acts on the normal direction between particles during in contact with each other.

Target Preparation: A target consists of 384,000 spherical particles with a radius of 1 mm (density 2.7 g/cm³, Young's modulus 94 GPa, Poisson's ratio 0.17). These particles are randomly fallen into a rectangular container with a base of 20 cm x 20 cm. We succeed in preparing 4 types of targets with a porosity of 43, 50, 62, and 72 % (Fig. 1), by changing adhesive force and rolling resistance of particles.

Simulation Settings: A projectile particle (density 2.7g/cm³, Young's modulus 70GPa, Poisson's ratio 0.35) impacts vertically into the target at velocities of $U=30, 100, \text{ or } 300 \text{ m/s}$. Gravity g is set to 1 or 10^{-4} G (cf. $g \sim 10^{-3} \text{ G}$ on Eros and 10^{-5} G on Itokawa). Corresponding to the two gravitational environments, we take $F_a=10^{-1} \text{ N}$ for 1 G and 10^{-5} N for 10^{-4} G ($F_a=10^{-5} \text{ N}$ for a 2 mm particle in general). The tensile strength of bulk targets estimated with Rumpf's equation [16] is $\sim 10^4 \text{ Pa}$ and $\sim 1 \text{ Pa}$ for $F_a = 10^{-1} \text{ N}$ and 10^{-5} N , respectively. The ratio F_a/F_g , where F_g is the gravity acting

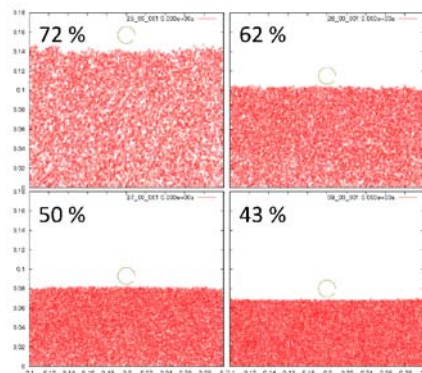


Figure 1: Cross sections of initial targets with various porosities (72, 62, 50, and 43%). A projectile ($r_p = 9 \text{ mm}$) is shown in each panel.

on single particle, is an index of influence of adhesion on the impact process [11] and are 10^3 for both cases. We also change projectile radius $r_p = 3$ or 9 mm. On the other hand, e and μ are fixed to 0.4 and 0.5, respectively. Adhesion is constant regardless of the targets and rolling resistance is not exerted during our impact simulation.

Results and Discussion: Figure 2 shows examples of snapshots of our simulations for cases with the same parameters of $r_p = 9$ mm, $U = 30$ m/s, $g = 10^{-4}$ G, and $F_a = 10^{-5}$ N. Observing all cases, as a whole, we see a general trend that penetration of (large) projectiles into highly porous targets makes long cavities with compressed walls.

When we assume a hydrodynamic force as a penetration resistance, the equation of motion of a projectile is given by

$$ma = (1/2)C_D \rho_t S v^2 - mg, \quad (1)$$

where m is the mass of a projectile, a is the acceleration, C_D is the drag coefficient, ρ_t is the target bulk density, S is the cross-section of projectile, and v is the penetration speed. Another form of this equation is

$$(8\rho_p/3\rho_t)r_p(a+g) = C_D v^2, \quad (2)$$

where ρ_p is the projectile density. We plotted LHS term of equation (2) as a function of $|v|$ in Figure 3. As a first order approximation, we obtained $C_D \sim 1-3$, independent of target porosity and parameters changed in this study. Such a resistance force is hydrodynamic and also appears in the previous impact experiments [13-15]. In terms of hydrodynamics, this means Reynolds number is large enough to give a constant C_D even in the porous granular targets.

Investigating the resistance force in more detail, we found that there is a term proportional to v

$$F' = -\beta \rho_t S v, \quad (3)$$

in addition to the hydrodynamic force (Fig.3). The coefficient β is about 5-10 m/s and seems independent of

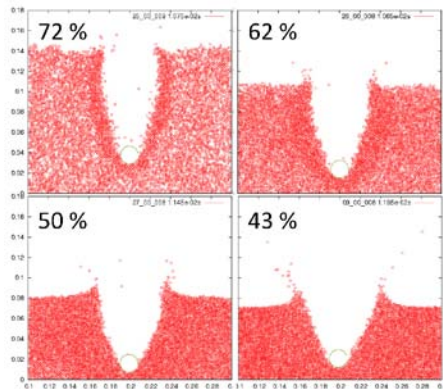


Figure 2: Snapshots of impacts into targets with different porosities at ~ 0.01 sec after impact ($r_p = 9$ mm, $U = 30$ m/s, $g = 10^{-4}$ G, and $F_a = 10^{-5}$ N).

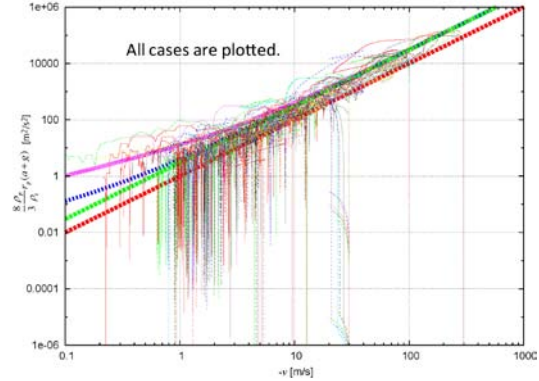


Figure 3: $(8\rho_p/3\rho_t)r_p(a+g)$ vs. $|v|$ for all cases. Thick broken lines represent reference lines: $y=|v|^2$ (red), $y=3/|v|^2$ (green), $y=3/|v|^2+|v|$ (blue), and $y=3/|v|^2+10/|v|$ (purple), where y denotes $(8\rho_p/3\rho_t)r_p(a+g)$.

target porosity and parameters in this study. This looks a kind of viscous resistance and could come from the particle interaction model we use in DEM calculation. Further investigation in a wider range of parameters is necessary in the future to affirm this resistance term.

A laboratory experimental study ongoing shows that the resistance force consists of two terms proportional to v^2 and v . The values of C_D and β are obtained as ~ 1 and ~ 3 m/s, respectively, from 70 m/s impact of a plastic sphere of 3 mm radius into a granular target with a porosity of 40 % consisting of glass beads of 50 μ m radius. Our numerical results are almost consistent with this experimental one.

Penetration process and its resistance law are critical when missions have plans of active impact experiments or interior explorations with penetrators. Our work will be also useful in planning such future asteroidal missions.

References: [1] Fujiwara A. et al. (2006) *Science*, 312, 1330-1334. [2] Saito J. et al. (2006) *Science*, 312, 1341-1344. [3] Miyamoto H. et al. (2007) *Science*, 316, 1011-1014. [4] Barnouin-Jha O. S. et al. (2008) *Icarus*, 198, 108-124. [5] Hirata N. et al. (2009) *Icarus*, 200, 486-502. [6] Michel P. et al. (2009) *Icarus*, 200, 503-513. [7] Housen K. R. and Holsapple K. A. (2003) *Icarus*, 163, 102-119. [8] Housen K. R. and Holsapple K. A. (2011) *Icarus*, 211, 856-875. [9] Yu A. B. et al. (2003) *Powder Technology*, 130, 70-76. [10] Scheeres D. J. et al. (2010) *Icarus*, 210, 968-984. [11] Wada K. et al. (2005) *LPS XXXVI*, Abstract #1596. [12] Cundall P. A. and Strack O. D. L. (1979) *G'eotechnique*, 29-1, 47-65. [13] Katsuragi H. and Durian D. J. (2007) *Nature Physics*, 3, 420-423. [14] Niimi R. et al. (2011) *Icarus*, 211, 986-992. [15] Okamoto T. et al. (2012) *LPS XLIII*, this issue. [16] Rumpf H. (1970) *Chemie Ingenieur Technik*, 42, 538-540.